Developmental Biology 373 (2013) 300–309

Contents lists available at SciVerse ScienceDirect

Developmental Biology

journal homepage: www.elsevier.com/locate/developmentalbiology

Thyroid hormone and retinoic acid interact to regulate zebrafish craniofacial neural crest development

Brenda L. Bohnsack, Alon Kahana *

Department of Ophthalmology and Visual Sciences, Kellogg Eye Center, University of Michigan, Ann Arbor, MI, USA

ARTICLE INFO

Article history:
Received 19 April 2012
Received in revised form
7 November 2012
Accepted 8 November 2012
Available online 17 November 2012

Keywords:
Craniofacial
Thyroid hormone
Neural crest
Migration
Pitx2
Twist1
Retinoic acid
Retinoid X receptor
Pharyngeal arch
Eye development

ABSTRACT

Craniofacial and ocular morphogenesis require proper regulation of cranial neural crest migration, proliferation, survival and differentiation. Although alterations in maternal thyroid hormone (TH) are associated with congenital craniofacial anomalies, the role of TH on the neural crest has not been previously described. Using zebrafish, we demonstrate that pharmacologic and genetic alterations in TH signaling disrupt cranial neural crest migration, proliferation, and survival, leading to craniofacial, extraocular muscle, and ocular developmental abnormalities. In the rostral cranial neural crest that gives rise to the periocular mesenchyme and the frontonasal process, retinoic acid (RA) rescued migratory defects induced by decreased TH signaling. In the caudal cranial neural crest, TH and RA had reciprocal effects on anterior and posterior pharyngeal arch development. The interactions between TH and RA signaling were partially mediated by the retinoid X receptor. We conclude that TH regulates both rostral and caudal cranial neural crest. Further, coordinated interactions of TH and RA are required for proper craniofacial and ocular development.

Introduction

Craniofacial and ocular congenital defects are often attributed to improper development of the cranial neural crest (CNC), a transient population of migratory embryonic stem cells. The CNC arises from neural ectoderm and forms numerous cell types, including bone, cartilage, and connective tissues of the craniofacial region, as well as corneal stroma and endothelium, iris stroma, ciliary body stroma and muscles, sclera, and trabecular meshwork of the eye (reviewed in Barembaum and Bronner-Fraser, 2005, Hong and Saint-Jeannet, 2005, Minoux and Rijli, 2010, Steventon et al., 2005, Trainor, 2005).

The molecular regulation of neural crest development is complex and involves numerous pathways that regulate induction from ectoderm, migration, survival, and differentiation (reviewed in Minoux and Rijli, 2010). CNC destined to form craniofacial structures either originates rostrally in the diencephalon and anterior mesencephalon or caudally in the posterior mesencephalon and hindbrain. The former gives rise to the frontonasal skeleton and CNC-derived structures in the ocular anterior segment, while the latter populates the pharyngeal arches (PA) that form the jaw, hyoid, and middle ear (Couly et al., 1993; Johnston, 1966; Kontges and Lumsden, 1996; Noden, 1983; Osumi-Yamashita et al., 1994). Anterior to posterior patterning of the CNC is established early through intrinsic homeodomain transcriptional programs (Depew et al., 2002, 2005; Hunt et al., 1991a, 1991b; Kimura et al., 1997; Kuratani et al., 1997; Matsuo et al., 1995; Stock et al., 1996) and maintained via cell–cell interactions with neighboring crest-free zones (Golding et al., 2002, 2004; Graham et al., 1993; Lumsden et al., 1991). CNC migration to the site of final destination and end differentiation are regulated by tissue-specific factors such as *twist1* in PAs (Soo et al., 2002) and *pitx2* in periocular and jaw mesenchyme (Dong et al., 2006; Evans and Gage, 2005; Gage et al., 1999; Kitamura et al., 1999).

Disruptions of CNC development lead to congenital craniofacial and ocular anomalies that together are coined "neurocristopathies" (Bolande, 1974). Although these disorders are typically associated with genetic mutations or chromosomal abnormalities, exposure to teratogens such as retinoic acid (i.e. isoretinoin) and alcohol give rise to craniofacial abnormalities (Deltour et al., 1996; Gitton et al., 2010; Lampert et al., 2003; Rosa et al., 1986; Sandell et al., 2007). Alterations in maternal or fetal thyroid hormone (TH) during pregnancy can result in craniofacial defects (Gamborino et al., 2001; Hirano et al., 1995; Israel et al., 1983). Congenital hypothyroidism or cretinism causes growth inhibition of the cranial base bone and cartilage resulting in a wide and short face with an underdeveloped mandible (Sperber et al., 2010). On the other hand, congenital hyperthyroidism causes craniosynostosis—the premature closure of cranial sutures leading to a misshapen head and potentially neurologic impairments (Hirano et al., 1995). Thus, tight regulation of TH levels during embryogenesis is important for craniofacial formation,

* Corresponding author. Fax: +1 734 615 0542.
E-mail address: akahana@med.umich.edu (A. Kahana).

0012-1606/$ - see front matter © 2012 Elsevier Inc. All rights reserved.
http://dx.doi.org/10.1016/j.ydbio.2012.11.005

but the molecular role of TH in CNC development has not been characterized.

TH synthesis and degradation are regulated by enzymes in thyroid follicles and target tissues. The chemically stable circulating form of TH, thyroxine (T4), is produced from thyroglobulin in thyroid follicles. In target tissues, 5′-deiodinase enzymes, DIO1 and DIO3, convert T4 to highly active, but unstable 3,3′,5-triiodo-L-thyronine (T3). The 5-deiodinase enzyme, DIO3, degrades T3 to inactive diiodo-L-thyronine (T2) as well as converts T4 to reverse 3, 3′–5′-triiodo-L-thyronine (rT3) (reviewed in Kohrle, 1999). It is thought that while DIO1 primarily contributes to systemic T3 synthesis, DIO2 activity occurs more locally, within individual microenvironments (Kohrle, 1999). Hence, DIO1-DIO3 and DIO2-DIO3 enzyme pairs form semi-independent mechanisms that regulate T3 levels systemically and locally, respectively.

Cellular effects of THs are classically mediated by thyroid receptor (TR) α and β, members of the nuclear hormone receptor superfamily. Following ligand binding, TRs heterodimerize with retinoid X receptor (RXR) and bind to DNA regulatory sequences. Recruitment of coactivators or corepressors regulates gene transcription (reviewed in Zhang and Lazar, 2000). Additional studies have shown that TH also acts through nongenomic pathways via integrin-mediated signaling and activation of tyrosine kinase receptors (Yonkers and Ribera, 2009).

In the current studies, we use zebrafish to study TH signaling in craniofacial development, utilizing the model's accessible and transparent embryos and availability of transgenic strains that mark the neural crest *in vivo*. In zebrafish, TRα has undergone gene duplication and *thraa* and *thrab* are expressed by 24 h post fertilization (hpf) (Thisse et al., 2001). In addition, *thraa* has at least two alternative splice variants (TRαA1 and TRαA1-2) (Takayama et al., 2008). The TRαA1-2 form has a C-terminal domain that shares homology to the human form and is the predominant variant expressed during embryogenesis (Takayama et al., 2008; Thisse et al., 2001). Although endogenous TH is not produced in follicles until 60 hpf, the yolk contains maternal stores. Using transgenic zebrafish, we characterized the effects of pharmacologically or genetically altering TH signaling on CNC migration, proliferation, and survival. We report that TH works alongside retinoic acid (RA) to regulate rostral and caudal CNC development, and that these interactions are critical for craniofacial and ocular development.

Materials and methods

Zebrafish care, mutants, and transgenics

Zebrafish (*Danio rerio*) were raised in a laboratory breeding colony on a 14 h light/10 h dark cycle as previously described (Bohnsack et al., 2011). Tg(*sox10::EGFP*), Tg(*foxd3::EGFP*) and Tg(*α-actin::EGFP*) strains were gifts of Thomas Schilling (Dutton et al., 2001), Mary Halloran (Curran et al., 2009), and Simon Hughes (Higashijima et al., 1997), respectively. Transgenic strains were crossed into *roy* background (White et al., 2008), a gift of Rachel Wong. 0.003% phenothiourea was added at 22 hpf to media of embryos harvested for *in situ* hybridization (Karlsson et al., 2001). Protocols have met guidelines for humane treatment of laboratory animals established by the University of Michigan Committee on the Use and Care of Animals, UCUCA protocol ♯10205.

Pharmacological treatment of embryos

Methimazole (Mthz; Sigma-Aldrich, St. Louis, MO) was directly diluted at the final concentrations as indicated (3–12 mM) in embryo media. Propylthiouracil (PTU; Sigma-Aldrich), T3 (Sigma-Aldrich), T4 (Sigma-Aldrich), rT3 (Sigma-Aldrich), all-trans RA (Sigma-Aldrich), and UVI3003 (Tocris Biosciences, Ellisville, MO) were diluted in DMSO at 1000x of final concentration and added to embryo media to final concentrations (PTU 0.05–0.1%; T3 100 nM; T4 100 nM; RA 0.01–1 nM; UVI3003 (1 nM–10 μM)) at indicated times. 0.1% DMSO served as control. Embryo media was changed every 24 h with fresh agents until embryos were harvested.

Morpholino oligonucleotides

Antisense morpholino oligonucleotides (MO) were synthesized by Gene Tools, LLC (Cowallis, OR) and dissolved in de-ionized water. MO sequence for Dio2 and p53 were previously published (Walpita et al., 2010, 2009). MO complementary to the start codons of Thraa (Thraa ♯1 and ♯2) and Dio3 were custom designed as was a 5 base pair mismatch control for the Dio3 MO (Table S1). MO concentrations (0.25 mM Thraa ♯1, 0.25 mM Thraa ♯2, 0.3 mM Dio2, 0.3 mM Dio3, 0.6 mM Dio3 Mismatch Control) that yielded consistent and reproducible phenotypes were determined. Control (globin) MO was injected with each experiment. MO sequences were lissamine-tagged for fluorescent tracking and comparison of embryos to insure similar amount of injected MO. 1 nL of MO (0.1–0.3 mM) was injected into the yolk of 1–2 cell stage embryos.

Functionality of Thraa and Dio3 MO was tested by coinjecting MO with mRNA encoding EGFP fused in frame with the MO target site. Briefly, EGFP was amplified from pCS2-EGFP (gift of David Turner) using T3 promoter primer for 3′ end and a custom primer which included SP6 promoter and MO sequence fused in frame to 5′end of EGFP coding sequence (Table S1). PCR product was purified and reamplified using SP6 and T3 primers. mRNA was transcribed using mMessage mMachine kit (Ambion Biosystems, Austin, TX), resuspended (100–200 ng/μL) and injected with or without respective MO at 1-cell stage. Injection of mRNA containing complementary sequence to MO resulted in diffuse GFP expression in the presence or absence of control MO. Co-injection of MO with corresponding mRNA abrogated GFP expression, demonstrating functionality of each MO (data not shown).

Embryos were analyzed with a Leica (Leica Microsystems CMS GmbH, Germany, Wetzler, Germany) M205FA combi-scope using a Leica DFC290 camera and the Leica Application Suite (LAS) (brightfield imaging), and a Hamamatsu ORCA-ER (Hamamatsu, Japan) camera with the Leica AF6000 software suite for fluorescent imaging.

Time-lapse imaging

12 hpf embryos were mounted in 1.5% low-melt agarose in a mounting chamber inside a Quick Exchange platform (QE-1, Warner Instruments, Hamden, CT) and covered in embryo media. Images were acquired with a Leica 25X water immersion objective on a Leica TCS SP5 MP multi-photon microscope fitted with a SpecraPhysics MaiTai DeepSee Ti-sapphire laser (Newport Corp., Irvine, CA). Images were obtained every 15 min until Prim-16 stage (~31 hpf). Images were processed with Leica LAS software and Adobe photoshop and sewn together using iMovie (Apple, Cupertino, CA).

In situ hybridization

In situ hybridization was performed as previously described (Barthel and Raymond, 2000; Bohnsack et al., 2011) using digoxigenin (Dig)-labeled RNA antisense probes. For colorimetric reactions and comparison of signal, embryos were developed for equal amounts of time. Embryos were cryoprotected and embedded in O.C.T. for sectioning. Sections were imaged with a Leica DM6000B Microscope using a Leica DFC500 camera.

Zebrafish ocular histology

Zebrafish embryos were fixed in 2% paraformaldehyde (PFA)/1.5% glutaraldehyde overnight at 4 °C then embedded in methylacrylate. Blocks were sectioned at 5 μm and sections were stained with Lee's stain or trichrome-like stain (Gruber, 1992; Prophet et al., 1992).

Reverse transcriptase-polymerase chain reaction

Zebrafish embryos were obtained at 36 hpf and RNA was isolated using the Fibrous Tissue RNeasy kit (Qiagen, Valencia, CA) and resuspended in diethylpyrocarbonate (DEPC)-treated water. RNA concentrations were measured by Nanodrop spectrophotometry (Thermo Scientific, Wilmington, DE). RNA was reverse transcribed using Superscript II (Invitrogen, Carlsbad, CA). Polymerase chain reaction (PCR) was performed using standard protocols and Platinum Taq (Invitrogen, Carlsbad, CA). The optimal annealing temperature and linear range of amplification cycles were determined for each primer pair (Table S2).

TUNEL assay

Zebrafish embryos were fixed in 4% PFA overnight at 4 °C and then cryoprotected in successive sucrose solutions (5%, 20%). Embryos were embedded in O.C.T. and sectioned at 10 μm. TUNEL assay was performed using standard protocols (ApopTag Red *In Situ* Apoptosis Detection Kit, Millipore, Billerica, MA). Briefly, sections were washed in PBS, refixed in 4% PFA, washed in PBS, incubated with equilibration buffer and then TdT enzyme for 1 h at 37 °C. Sections were washed in Stop/Wash buffer and PBS then incubated with blocking solution and rhodamine-conjugated Anti-Dig antibody for 1 h at room temperature. Sections were washed in PBS, co-stained with Dapi (Invitrogen) and visualized using epifluorescence microscopy. For quantification, 3 consecutive sections through the equator of the lenses and 1 section just posterior to the eye of 4 embryos were included in the analysis. Cell nuclei and TUNEL positive cells were counted manually and with ImageJ (National Institutes of Health, Bethesda, MD). Student's *t*-test were performed and $p < 0.05$ was considered statistically significant.

Immunostaining

Zebrafish embryos were fixed in 4% PFA overnight at 4 °C and then cryoprotected in successive sucrose solutions. Embryos were embedded in O.C.T. and sectioned at 10 μm. Sections were washed in PBS, blocked in 10% normal goat serum in PBS-1% triton-X for 1 h at room temperature, and then incubated in rabbit Anti-Phosphohistone *H3* (Ser10; 1:500; Cell Signaling Technology, Boston, MA) for 1 h at room temperature. Embryos were washed in PBS, incubated with Goat anti-Rabbit IgG conjugated with Cy3 (1:500, Abcam, Cambridge, MA) for 1 h at room temperature. Sections were washed in PBS, costained with Dapi, and then visualized using epifluorescence microscopy. For quantification, 3 consecutive sections through the equator of the lenses and 1 section just posterior to the eye of 4 embryos were included in the analysis. Cell nuclei and cells expressing phosphohistone-H3 were counted manually and with ImageJ (National Institutes of Health, Bethesda, MD). Student's *t*-test were performed and $p < 0.05$ was considered statistically significant.

Results

Goitrogens inhibit CNC development

Methimazole (Mthz) inhibits conversion of T4–T3 while propylthiouracil (PTU) inhibits formation of T4 from thyroglobulin as well as conversion of T4–T3. We treated embryos with increasing concentrations of Mthz or PTU at different time points using transgenic strains that express GFP in CNC [Tg(*sox10::EGFP*)] or differentiated muscle [Tg(α-*actin::EGFP*)]. Mthz (3 mM) starting at 10 hpf (prior to CNC migration) altered jaw formation at 96 hpf, with formation of Meckels cartilage (1st PA), but not ceratohyal cartilage (2nd PA); Fig. S1A vs. Fig. S1E, I, J). Higher concentrations (>6 mM) starting at 10 hpf resulted in death by 72 hpf (data not shown). Increasing concentrations starting at 22 hpf (3–6–9 mM, Fig. S1B/F, C/G, D/H, respectively) progressively inhibited PA and jaw cartilage development but had minimal effect on craniofacial muscles. At higher concentrations (>12 mM), Mthz starting at 22 hpf resulted in death by 72 hpf (Table S3).

Treatment with 0.05% PTU starting at 10 hpf caused mild deformation and inferior displacement of ceratohyal cartilage (Fig. S2A) vs. 0.1% DMSO (Fig. S2D), but had minimal effect on PA or craniofacial muscle development (Table S3). Treatment with higher concentrations at 10 hpf caused death (data not shown). Starting at 22 hpf, 0.05% PTU had minimal effect on neural crest development (Fig. S2B), but 0.075% caused mild ceratohyal cartilage abnormalities (Fig. S2C) and 0.1% caused death by 72 hpf (data not shown). Co-treatment with exogenous T3 (100 nM) and T4 (100 nM) did not rescue PTU-induced defects and in fact caused loss of the 7th PA at higher concentrations of PTU (Fig. S2E, F). Similarly, exogenous T3 and T4 did not rescue Mthz (3–9 mM)-induced defects (data not shown). Treatment with T3 and T4 alone caused mild frontal bossing and subtle inferior displacement of ceratohyl cartilage (Fig. S2G and data not shown).

Thraa is required for CNC and extraocular muscle development

Since Mthz and PTU-induced defects were not rescued by exogenous TH, we further investigated the role of TH signaling on craniofacial development by using MOs that inhibited Thraa translation. The *thraa* gene is expressed in the developing neural crest (Takayama et al., 2008; Thisse et al., 2001). Thraa knockdown inhibited neural crest migration as evidenced by lack of GFP expressing cells in Tg(*foxd3::EGFP*) embryos (Fig. 1B, E vs. A, D) and disruption of *crestin* expression by *in situ* hybridization (Fig. 1H, K vs. G, J). Thraa knockdown completely inhibited rostral CNC migration ventral to the eye and mildly disrupted CNC migration dorsal to the eye (Video 2). This is in contrast to control embryos (Video 1) in which rostral CNC migrated in a dorsal wave (destined to become frontonasal skeleton) and in a ventral wave (contributes to frontonasal process and components of the anterior segment of the eye). Thraa knockdown resulted in malformation of Meckels and ceratohyal cartilages, as seen by *in vivo* imaging in Tg(*sox10::EGFP*) larvae (Fig. 2B vs. 2A), *col2a1 in situ* hybridization (Fig. 2E vs. 2D), and methylacrylate section histology (Fig. 2K vs. 2J) at 96 hpf. Furthermore, by 96 hpf *foxd3* is predominantly expressed in photoreceptors in control embryos (Fig. 2G), but this was decreased by Thraa knockdown (Fig. 2H). Thraa also regulated development of CNC-derivatives in the ocular anterior segment (Fig. 2N, Q vs. M, P). Co-injection of p53 MO with Thraa MO (Fig. S3B) caused malformation of Meckels and ceratohyal cartilages compared to embryos injected with control MO (Fig. S3D) or p53 MO alone (Fig. S3A) demonstrating that the effect of Thraa knockdown was not due to nonspecific apoptosis. In addition, Meckels and ceratohyal cartilage formation

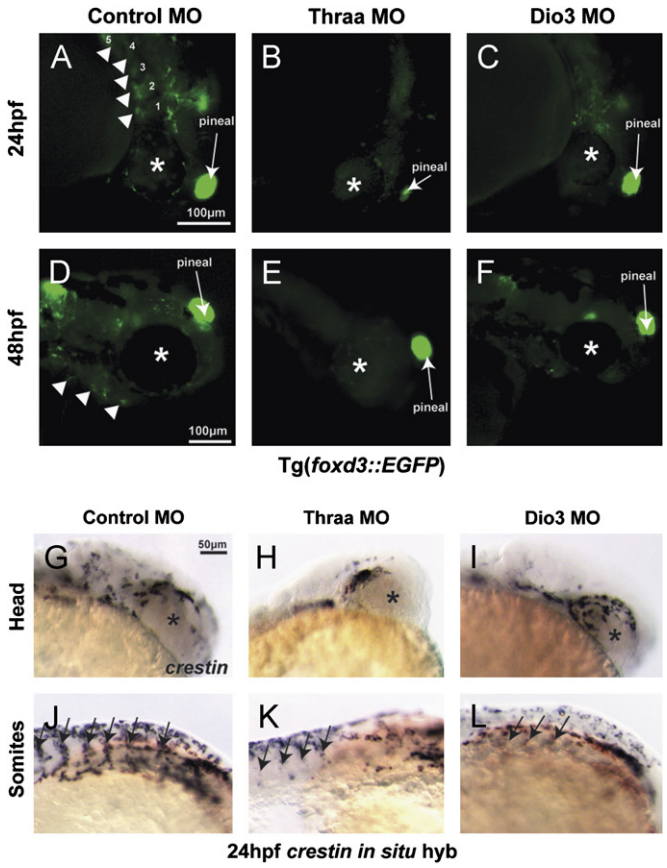

Fig. 1. TH regulates early neural crest development. Thraa MO knockdown (decreased TH signaling) inhibited neural crest migration at 24 (B) and 48 hpf (E) vs. control (A, D) in Tg(*foxd3::EGFP*). Thraa MO knockdown inhibited expression at 24 hpf of *crestin* in the head (H) and body (K; between somites, arrows) vs. control (G, J). Dio3 MO knockdown (increased TH) in Tg(*foxd3::EGFP*) embryos inhibited PA (arrowheads) formation at 24 (C vs. A) and 48 hpf (F vs. D). *In situ* hybridization for *crestin* demonstrated Dio3 MO knockdown impaired neural crest migration in the head (I) and between somites (L, arrows) at 24 hpf. Asterisk denotes developing eye. Scale bar=50 or 100 μm as indicated.

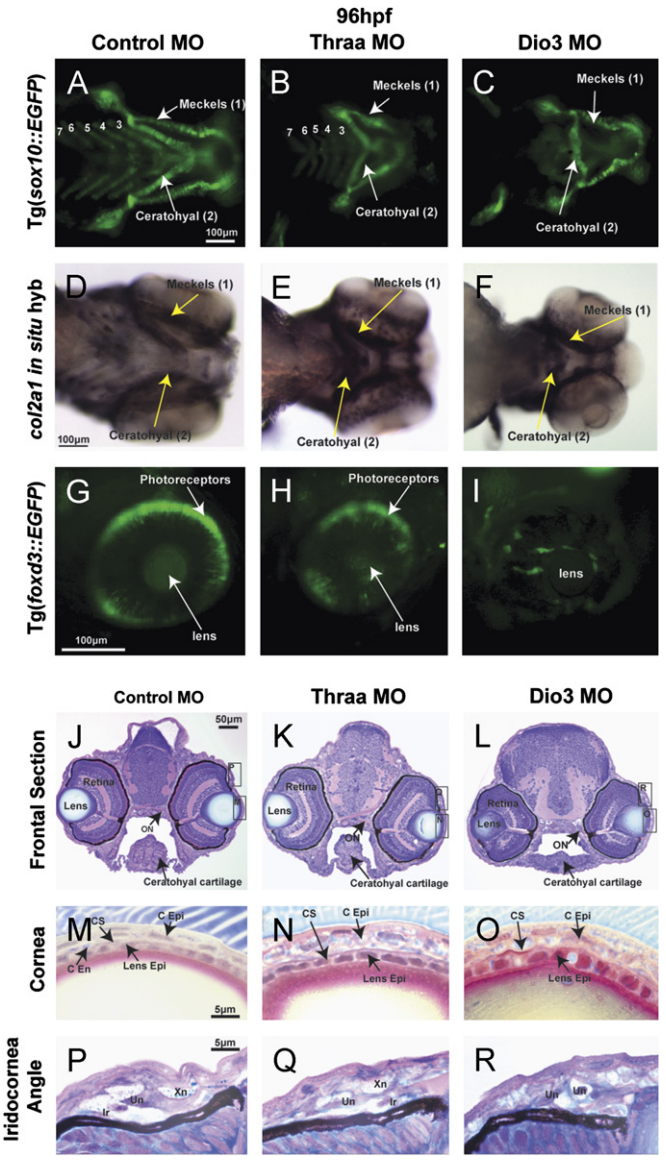

Fig. 2. TH is required for craniofacial and ocular development. 96 hpf control embryos demonstrated neural crest-derived structures including 7 PAs (Meckels cartilage (1st PA), ceratohyal cartilage (2nd PA), and 5 posterior PAs) *in vivo* in Tg(*sox10::EGFP*) zebrafish (A) and by *col2a1 in situ* hybridization (D). Control embryos also showed *foxd3* expression in photoreceptors at 96 hpf Tg(*foxd3::EGFP*) embryos (G). Thraa MO knockdown inhibited Meckels and ceratohyal cartilage formation, decreased the number of posterior PAs (B, E), and decreased photoreceptor expression of *foxd3* (H). Dio3 MO knockdown inhibited posterior PA formation (C, F) and *foxd3* expression in photoreceptors (I). Dio3 MO knockdown had less effect on Meckels and ceratohyal cartilage formation. Methylacrylate sections demonstrated that control embryos (J) had corneas (M) that contained epithelial (C Epi), stromal (C S), and endothelial (C End) layers, lens epithelial cells (Lens Epi) adjacent to the cornea, and iris stroma with xanthophores (Xn), iridophores (Ir), and undifferentiated cells (Un). Thraa MO knockdowns (K, N, Q, T) demonstrated thickened and scalloped C Epi, lack of C End (N) and decreased cellularity of the iridocorneal angle (Q) vs. control (J, M, P). ON, optic nerve; MR, medial rectus. Scale bar=5, 10, 50 or 100 μm as indicated.

was also inhibited by a second translation blocking MO against Thraa (Fig. S3B vs. A) demonstrating replication of phenotype.

Supplementary material related to this article can be found online at doi:10.1016/j.ydbio.2012.11.005.

We have previously demonstrated that post-migratory CNC cells are required for extraocular muscle (EOM) organization (Bohnsack et al., 2011). Thus, we next investigated whether MO knockdown of Thraa affected craniofacial myogenesis and specifically EOM formation. MO knockdown of Thraa did not disrupt muscle differentiation, but caused indistinct EOMs (Fig. 3B, E, H, J vs. A, D, G, I) constituting an intermediate muscle phenotype. These results suggest that Thraa-mediated signaling is important for CNC development, consistent with the partial migratory phenotype and cartilage malformations (Table S4).

Altering TH signaling via deiodinase-3 gene knockdown affects craniofacial development

We next investigated whether alterations in TH levels affected craniofacial development. *Dio1* is expressed in the liver while *dio2* is expressed in the developing retina (Thisse et al., 2001). MO knockdown of Dio2 mildly decreased the expression of *tyrosinase*, a target of TH signaling (Walpita et al., 2009) (Fig. S4A, B vs. E, F) and resulted in mild delay of CNC-derived jaw and PA cartilage formation at 72 hpf (Fig. S5B vs. A). The delay was rescued by 100 nM T3 (Fig. S5D), but not 100 nM rT3 (Fig. S5F). Treatment of control embryos with exogenous 100 nM T3 caused a frontal "bossing" effect (data not shown) but had no effect on jaw and PA formation (Fig. S5C). Exogenous 100 nM rT3 had no effect on craniofacial development of control embryos (Fig. S5E). Delay in jaw and PA cartilage development in Dio2 MO knockdowns was no longer present at 96 hpf (Fig. S5G, H and Fig. S6A). Furthermore, MO knockdown of Dio2 did not affect anterior segment (Fig.S6B, C) or craniofacial muscle development (Fig. S5I, J and Fig. S6D).

Dio3, which degrades T3 to T2 and converts T4 to rT3, was strongly expressed in the pronephros (Fig. S7A, B, D, E, G, H, J, K) and weakly in the head (Fig. S7C, F, I, L). MO knockdown of Dio3, which increased *tyrosinase* expression by *in situ* hybridization (Fig. S4C, D) and semi-quantitative RT-PCR (Fig. 4Y), did not disrupt early migration of neural crest cells expressing *foxd3* (Fig. 1C), but did inhibit segregation of caudal neural crest into distinct PAs (Fig. 1F). *Crestin in situ* hybridization further demonstrated improper CNC migration into the head and between somites in Dio3 MO knockdowns (Fig. 1I, L).

Time-lapse microscopy of Dio3 MO knockdown embryos revealed that ventral CNC wave initiated migration around the eye, but halted mid-track and migrated toward the neck instead of converging with the dorsal wave (Video 3). Thus in Dio3 knockdowns, impaired caudal CNC development inhibited development of posterior PAs, ceratohyal cartilage (Fig. 2C, F, L), iris stroma (Fig. 2I) and the anterior segment (Fig. 2O, R), Further, MO knockdown of Dio3 inhibited photoreceptor expression of *foxd3* (Fig. 2I). Co-injection of p53 and Dio3 MOs (Fig. S3C) or injection of Dio3 mismatch MO (Fig. S3F) also inhibited posterior PA and ceratohyal cartilage formation demonstrating the phenotype was not secondary to nonspecific apoptosis or nonspecific MO effects. Exogenous 100 nM T3 or 100 nM rT3 starting at 6 hpf did not rescue CNC defects in Dio3 MOs (data not shown). MO knockdown of Dio3 did not affect early muscle differentiation at (Fig. 3L, N vs. K, M), but EOMs were indistinct with thickened, overlapping insertions by 96 hpf (Fig. 3C, F). Thus, increased TH signaling disrupted CNC and EOM development (Table S4).

Supplementary material related to this article can be found online at doi:10.1016/j.ydbio.2012.11.005.

TH regulates expression of genes important in craniofacial development

We next asked whether alterations in TH signaling affected genes associated with human congenital craniofacial disorders. *Twist1*, a basic helix–loop–helix transcription factor, regulates neural crest migration, and haploinsufficiency causes Saethre–Chotzen Syndrome (el Ghouzzi et al., 1997; Howard et al., 1997). Zebrafish contains two paralogs of *TWIST1*, termed *twist1a* and *1b* (Germanguz et al., 2007; Yeo et al., 2007), and we chose to focus on *twist1a* for this study. During normal zebrafish development, *twist1a* is expressed from 24 to 48 hpf in PAs with the greatest amount in primordial Meckels and ceratohyal cartilages (Fig. 4A, D). Alterations in TH signaling (via MO knockdown of Thraa or Dio3) did not alter overall expression of *twist1a* in RNA derived from whole 36 hpf embryos (Fig. 4Y), but appeared to alter the pattern of expression in the PA by *in situ* hybridization (Fig. 4B, C, E, F).

We also assessed the effect of TH on *pitx2,* a homeobox transcription factor associated with Axenfeld–Rieger Syndrome. In 48 hpf control embryos (Fig. 4G, J), *pitx2* was expressed in periocular mesenchyme (POM), EOMs (double arrows), jaw (arrows), and pituitary (small arrowheads). Decreased TH (Thraa MO) signaling and increased TH (Dio3 MO) signaling did not alter overall *pitx2* expression in RNA from whole embryos (Fig. 4Y), but *in situ* hybridization appeared to show decreased expression in the POM (Fig. 4H, K vs. G, J and Fig. 4I, L vs. G, J). These results

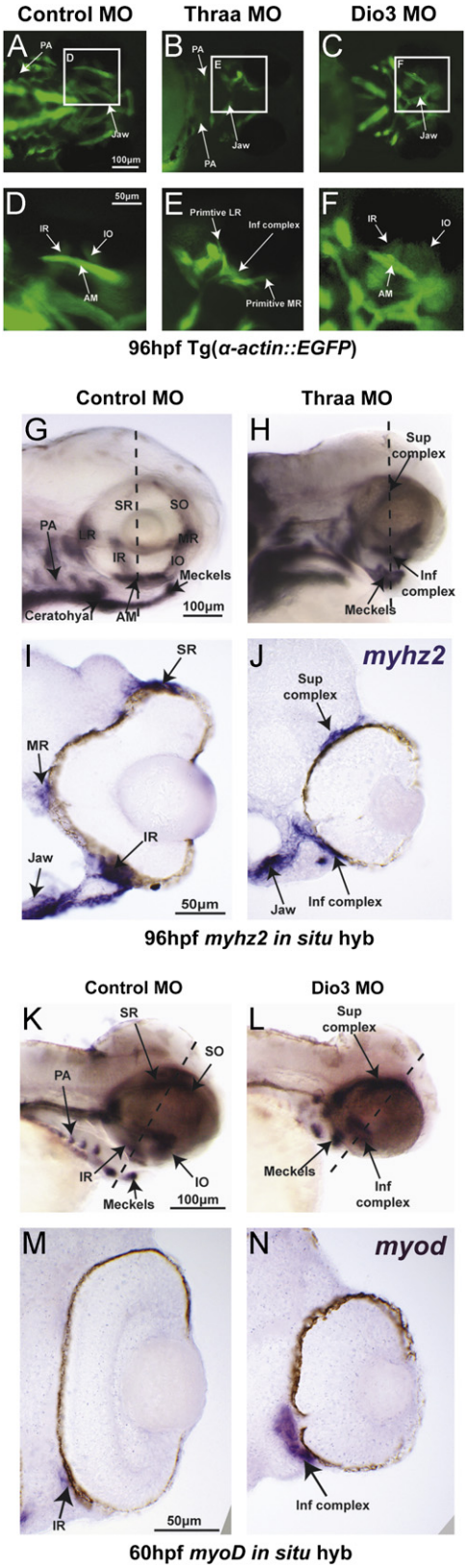

Fig. 3. TH regulated craniofacial muscle development including EOM organization. 96 hpf control embryos demonstrated 6 distinct EOM; medial rectus (MR), lateral rectus (LR), superior rectus (SR), superior oblique (SO), inferior rectus (IR), and inferior oblique (IO) *in vivo* in Tg(α-*actin::EGFP*) (A, D) and by *in situ* hybridization for *myzh2* (G, I). *In situ* hybridization for *myoD* demonstrated early muscle differentiation in EOM at 60 hpf (K, M). Thraa MO knockdown inhibited jaw and PA muscle development (B, H). Thraa MO knockdown did not disrupt muscle differentiation, but caused indistinct superior (sup) and inferior (inf) EOM complexes (E, H, J). Dio3 MO knockdown inhibited posterior PA development (C, L) and caused thickening and overlapping of EOM insertions (F). At 60 hpf EOMs in Dio3 MO knockdowns showed early muscle differentiation (L), but were clustered together and indistinct in wholemount (L) or on sections (N). AM, anterior mandibulae. Scale bar=50 or 100 μm as indicated.

reveal that altered TH signaling disrupted CNC migration and development and altered expression of transcription factors associated with human congenital craniofacial maldevelopment.

Because of known interactions between PitX2 and retinoic acid (RA) and the critical role of RA signaling in craniofacial development, we next investigated whether TH influenced expression of enzymes that synthesize (*retinaldehyde dehydrogenase*) or degrade (*cytochrome P450*) RA. In control embryos, *raldh2* was expressed in dorsal retina with a small amount also in ventral retina at 24 hpf (Fig. S8A, C). At 36 hpf (Fig. S8B, D) and 48 hpf (Fig. 4M, P), *raldh2* was expressed in the retina and in the jaw, PAs, and POM. Thraa MO knockdown (decreased TH signaling), decreased *raldh2* expression by RT-PCR in RNA derived from whole 36 hpf embryos (Fig. 4Y). *In situ* hybridization demonstrated decreased *raldh2* expression in the ventral retina, jaw, and brain at 48 hpf (Fig. 4N, Q). MO knockdown of Dio3 (increased TH signaling) did not affect overall *raldh2* expression in RNA from whole 36 hpf embryos (Fig. 4Y), but *in situ* hybridization demonstrated a localized decrease in jaw, PAs, and POM (Fig. 4O, R) at 48 hpf. *In situ* hybridization for cytochrome P450 genes *cyp26a1* and *cyp26b1* revealed no difference in expression at 48 hpf (data not shown). As previously described by McCaffery et al., *cyp26c1* expression demarcates the dorsal and ventral retina in control embryos at 24 (Fig. S8E), 36 (Fig. S8F), and 48 hpf (Fig. 4S, V). In addition, *cyp26c1* was expressed in otic vesicles and later in the jaw. Semi-quantitative RT-PCR of 36 hpf whole embryo RNA demonstrated that alterations in TH signaling (Thraa MO or Dio3 MO) did not change overall expression (Fig. 4Y). *In situ* hybridization showed localized increase in *cyp26c1* expression in the otic vesicle and nasal pit (Fig. 4T, W) in Thraa MO embryos even when compared with 24 hpf control embryos (Fig. S8E). On the other hand, increased TH signaling (via Dio3 MO knockdown) increased expression of *cyp26c1* in retina and hindbrain (Fig. 4U, X). Taken together, TH signaling during early CNC development regulates craniofacial RA synthesis and degradation in a region-specific fashion, suggesting a mechanism of action for TH signaling.

TH and RA have reciprocal effects on CNC development

RA, like TH, signals through nuclear hormone receptors (RA receptors; RAR) to regulate gene expression. Because of the close relationship between RARs and TRs as well as our finding that alterations in TH signaling disrupted regulation of RA synthesis and degradation, we investigated interactions between these pathways.

Following knockdown of Thraa expression (blocking TH signaling, Fig. 5E), addition of 1 nM RA starting at 12 hpf (beginning of CNC migration) improved Meckels and ceratohyal cartilage formation at 96 hpf (Fig. 5F) and restored migration of ventral wave rostral CNC (Video 4) revealing that increased RA signaling compensated for reduced TH signaling in the 1st and 2nd PAs. Treatment of Dio3 knockdown (leading to excess TH signaling, Fig. 5I) embryos with 1 nM RA starting at 12 hpf improved caudal

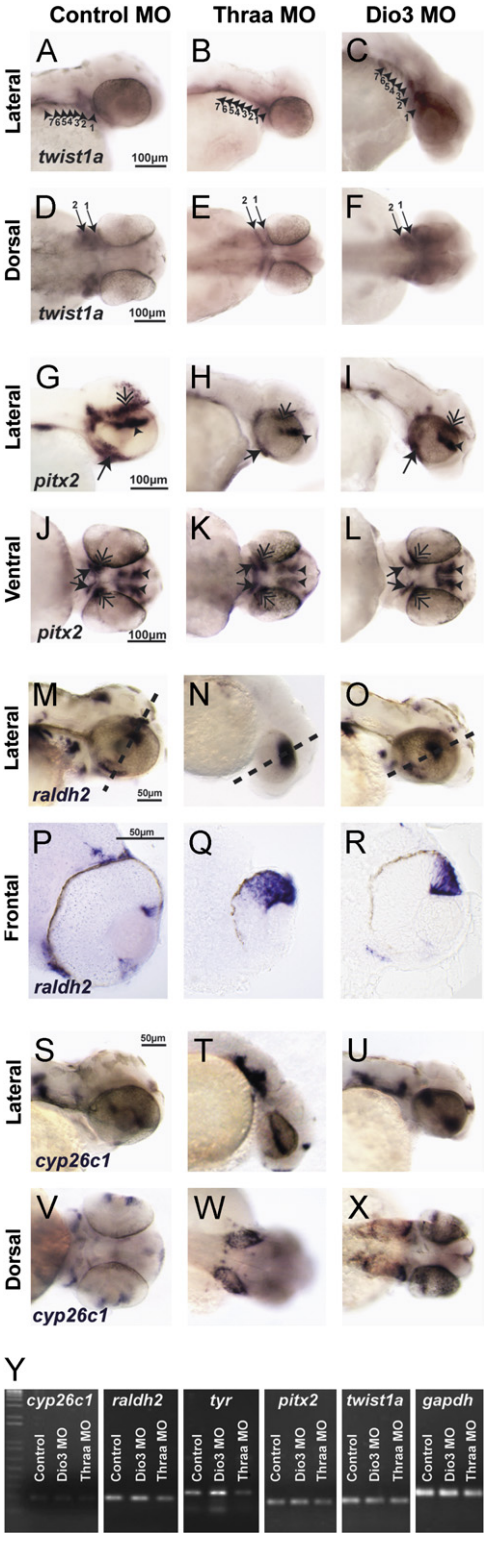

Fig. 4. TH regulates expression of *twist1a* and *pitx2.* 48 hpf expression of *twist1a* by *in situ* hybridization demonstrated decreased expression in Thraa MO knockdowns (B, E) which was expressed in pharyngeal arches (arrowheads) in controls (A, D). Increased TH (via MO knockdown of Dio3) demonstrated increased expression of *twist1a* within pharyngeal arches (C, F, arrowheads). *In situ* hybridization for *pitx2* demonstrated markedly decreased expression in periocuar mesenchyme of Thraa MO knockdowns (H, K, double arrowheads) and slightly decreased expression in POM of Dio3 (I, L, double arrowheads) MO knockdown. *Pitx2* was normally expression in the jaw (arrows), POM (double arrowheads), optic nerve (large arrowheads) and pituitary (small arrowheads) in control embryos (G, J). *In situ* hybridization demonstrated in control embryos that *raldh2* was expressed in ventral and dorsal retina, jaw, and POM at 48 hpf (M, P). In Thraa MO knockdowns, *raldh2* was only expressed in the dorsal retina at 48 hpf (N, Q). MO knockdown of Dio3 decreased expression of *raldh2* in pharyngeal arches and POM (O, R). *In situ* hybridization in control embryos demonstrated expression of *cyp26c1* in a demarcating line between dorsal and ventral retina, hindbrain, and otic vesicle 48 hpf (S, V). MO knockdown of Thraa (T, W) and Dio3 (U, X) increased expression of *cyp26c1* in the retina, hindbrain, and otic vesicle. Scale bar = 50 μm. Semi-quantitative RT-PCR of RNA (Y) derived from whole 36 hpf control, Dio3 MO, or Thraa MO demonstrated no difference in expression of *cyp26c1*, *pitx2*, and *twist1a.* RT-PCR demonstrated decreased overall expression of *raldh2* and *tyrosinase* (*tyr*) in Thraa MO compared to control. Dio3 MO knockdown showed increased expression of *tyr*. Semi-quantitative RT-PCR used Gapdh and S18 (data not shown) as internal controls.

CNC-derived posterior PA formation, but suppressed Meckels cartilage development at 96 hpf (Fig. 5J) revealing that increased RA signaling improved posterior arch development at the expense of anterior arches. Time-lapse imaging revealed that rostral CNC migrated ventral to the eye, but cellular movement was disorganized when excess TH was combined with excess RA (Dio3 knockdown+1 nm RA; Video 5). Treatment of control embryos with 1 nM RA demonstrated initiation of migration and impaired ventral wave maintenance (Video 6), but only minimal teratogenic effects on jaw and PA development (Fig. 5B vs. A). Thus, the relative balance of TH and RA signaling shifts developmental programs between anterior and posterior PA formation.

Supplementary material related to this article can be found online at doi:10.1016/j.ydbio.2012.11.005.

We further probed interactions between RA and TH by testing whether RXR, a shared heterodimeric partner, mediated these interactions in CNC. Treatment of control embryos starting at 12 hpf with high dose RXR antagonist UVI3003 (>1 μM) resulted in death by 96 hpf (data not shown). 10 nM UVI3003 in the absence (Fig. 5C) or presence (Fig. 5D) of 1 nM RA did not significantly affect cranial neural crest development.

Following blocking of TH signaling via Thraa knockdown, treatment with 10 nM UVI3003 decreased the number of PAs from 7 to 6 (Fig. 5G). Concentrations of UVI3003 higher than 100 nM caused death (data not shown). We then found that UVI3003 abrogated the ability of RA to rescue anterior arch formation following Thraa knockdown (Fig. 5H).

Next we tested the effect of UVI3003 in the context of excess TH signaling (via Dio3 knockdown). We found that adding 10 nM UVI3003 to Dio3 knockdown embryos improved posterior PA and ceratohyal cartilage development (Fig. 5K). However, when 1 nM RA and 10 nM UVI3003 were added together to Dio3 knockdown embryos, a worse craniofacial phenotype with complete lack of PA formation was observed (Fig. 5L).

We conclude that in caudal CNC development, RXR mediates between TH and RA signaling, while in the rostral CNC, RA functions downstream of TH in the regulation of ventral wave migration.

TH and RA regulate cellular proliferation and apoptosis

We next tested whether TH and RA altered CNC proliferation and cell survival. Decreased TH signaling (Thraa MO knockdown) did not affect the overall percent of cells in M phase (21% ± 1% vs. 17.8% ± 0.05%, Fig. 6G) as detected by immunostaining for phosphorylated phosphohistone-H3 (Ser 10) in 36 hpf embryos (Fig. 6B vs. A). However, there were significantly ($p<0.0001$) fewer cells in sections derived from 36 hpf Thraa embryos (778.0 ± 211.8) compared to control (1272.4 ± 226.5, Fig. S9). Treatment with 1 nM RA did not alter the percent of cells in *M* phase in Thraa MO knockdown embryos (17% ± 8%, Fig. 6E) or control embryos (18% ± 5%, Fig. 6D) and did not significantly change the total number of cells in Thraa MO knockdown embryos (854.5 ± 280.7) or control embryos (1338.3 ± 241.3). Increased TH signaling (Dio3 MO knockdown) significantly increased the percent of cells in M phase (31.6% ± 0.06%; Fig. 6C, $p<0.0001$) and decreased the total number of cells in each section (1092.1 ± 194.7, $p<0.01$). Treatment of Dio3 knockdown embryos with 1 nM RA did not alter the percent of cells in

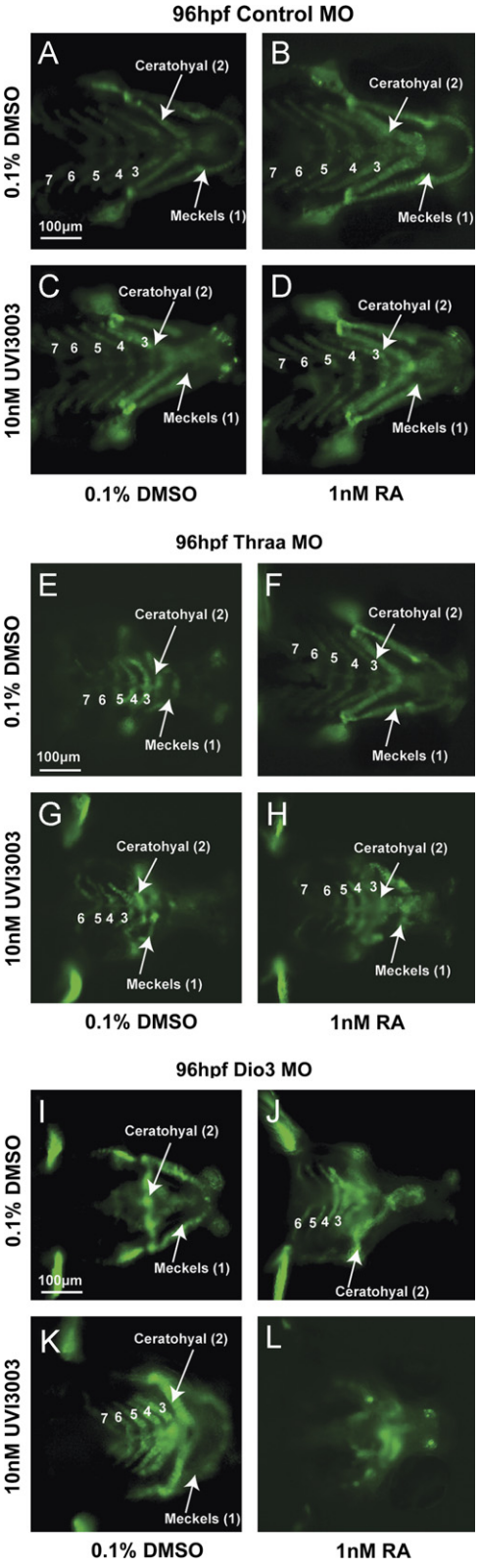

Fig. 5. RA and TH have reciprocal interactions on caudal neural crest development that are mediated by RXR. Treatment of Tg(*sox10::EGFP*) embryos injected with control MO with 1 nM RA starting at 12 hpf had minimal teratogenic effects (B) vs. control media (A). Treatment with RXR antagonist, 10 nM UVI3003 in the absence (C) or presence of 1 nM RA (D) had minimal affect on cranial neural crest development. MO knockdown of Thraa caused malformation of ceratohyal and Meckels cartilage formation (E) which was rescued by 1 nM RA (F) starting at 12 hpf. In contrast, treatment with UVI3003 (10 nM) at 12 hpf further inhibited Meckels, ceratohyal, and posterior PA cartilage (G) and abrogated the effect of exogenous RA (H) on Thraa MO knockdowns. MO knockdown of Dio3 inhibited posterior PA formation (I) which was improved by exogenous RA (1 nM, J) starting at 12 hpf. 10 nM UVI3003 starting at 12 hpf improved posterior pharyngeal arch and ceratohyal cartilage in Dio3 MO knockdowns (K), however, co-treatment with 10 nM UVI3003 and 1 nM RA completely suppressed pharyngeal arch and jaw development (L). Scale bar=100 μm.

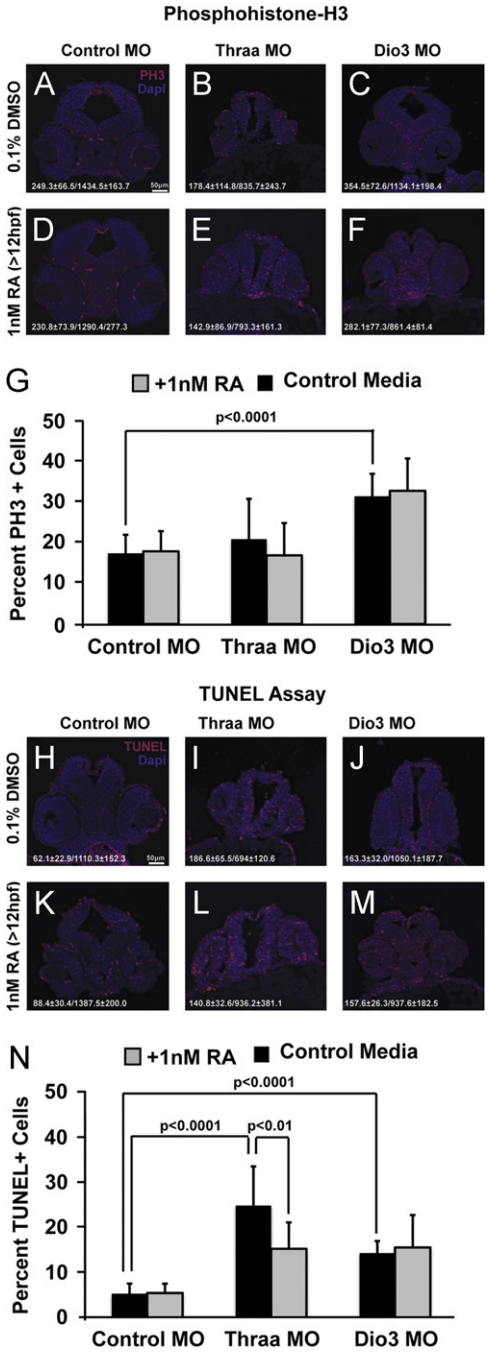

Fig. 6. TH is required for cell proliferation and survival. Immunofluorescence for phosphohistone H3 (PH3), a marker for M phase demonstrated no significant difference in the percent of proliferating cells in Thraa MO knockdowns (B) compared to control (A,G). The average numbers of PH3 positive cells and total nuclei are given for each group ($n=4$), There was a significant increase in percent of proliferating cells in Dio3 MO knockdown embryos (C, D, $p<0.0001$). Treatment with exogenous 1 nM RA starting at 12 hpf did not affect the percent of proliferating cells in controls (D), Thraa MO (E), or Dio3 MO (F). TUNEL assay demonstrated a significant increase in percent of apoptotic cells in Thraa MO (I, $p<0.0001$)) and Dio3 MO (J, $p<0.0001$) compared to controls (H, N). The average numbers of TUNEL positive cells and total nuclei are given for each group ($n=4$). Treatment with 1 nM RA starting at 12 hpf significantly decreased the percent of apoptotic cells in Thraa MO (L, $p<0.01$). Exogenous RA did not affect the percent of apoptotic cells in controls (K) or Dio3 MO (M). Scale bar=50 μm.

M-phase ($33\% \pm 8\%$, Fig. 6E), but did significantly decrease ($p<0.01$) the total number of cells per section (900.0 ± 144.3 vs. 1092.1 ± 194.7).

To assess cell survival, we utilized the TUNEL assay to ask whether TH and RA regulated CNC apoptosis. Blocking TH signaling (Thraa knockdown) significantly ($p<0.0001$) increased the percent of cells that were apoptotic at 36 hpf ($27.5\% \pm 10\%$ vs. $6.0\% \pm 2.5\%$, Fig. 6I vs. H, N). Treatment of Thraa MO knockdown with 1 nM RA significantly decreased the percent of apoptotic cells ($16.9\% \pm 6.5\%$, Fig. 6L, $p<0.01$). Treatment of control embryos with 1 nM RA did not significantly alter the percent of apoptotic cells ($6.0\% \pm 2.3\%$, Fig. 6K). Increased TH signaling (Dio3 knockdown) also significantly increased the percent of apoptotic cells ($15.8\% \pm 3\%$, Fig. 6J). Treatment of Dio3 MO knockdowns with 1 nM RA did not change the percent of apoptosis ($17.2\% \pm 8\%$, Fig. 6M).

We conclude that TH is required for maintaining cellular proliferation during CNC development, but sustained levels of TH appeared to prevent cells from exiting the cell cycle, suggesting that local transition from high TH to low TH via Dio3 activity is important in final stages of CNC migration and early differentiation.

Discussion

Early patterning of CNC as it originates from neuroectoderm establishes the pharyngeal region and head mesenchyme and lays the foundation for craniofacial development (Betancur et al., 2010; Couly et al., 1993; Johnston, 1966; Minoux and Rijli, 2010; Noden, 1983). Intrinsic transcription factor-mediated pathways and extrinsic signals are required for proper neural crest development. We now report that TH signaling is required for rostral and caudal CNC development, revealing a complex interplay between TH and RA in establishing rostro-caudal and dorso-ventral CNC patterning (Fig. 7).

Although maternal hyper- and hypothyroidism have been associated with congenital defects (Gamborino et al., 2001; Hirano et al., 1995; Israel et al., 1983), the role of TH during embryogenesis has not been well described. In mice, mutation and deletion of TRs had minimal effects on development (Gothe et al., 1999), suggesting that embryogenesis may involve non-genomic TH signaling (Yonkers and Ribera, 2009). In contrast, in zebrafish Thraa is required for CNC migration, proliferation, survival and differentiation. This disparity likely represents differences in compensatory signaling systems between zebrafish and murine models, including possibility of overlapping functions among different hormone receptors.

Our studies demonstrate the important role of TH signaling in regulating caudal and rostral CNC development (Fig. 7). While intrinsic *hox* and *dlx* transcription factors demarcate streams of

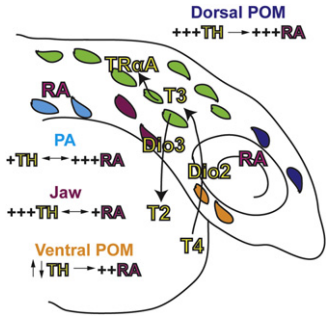

Fig. 7. Model of TH and RA in regulating craniofacial neural crest. TH and RA are both required for neural crest cell migration into the head region (A). Craniofacial tissues have a range of sensitivities to TH and RA (B). Posterior pharyngeal arch (PA) development requires low levels of TH and high levels of RA while jaw formation is dependent on higher levels of TH and lower levels of RA. Further interactions between TH and RA are partially mediated by RXR in both posterior PA and jaw development. RA is downstream of TH in regulation of neural crest migration dorsal and ventral to the eye to form the periocular mesenchyme (POM) and frontonasal process. Initiation of ventral POM migration is dependent on TH, but then requires Dio3-mediated TH degradation for completion of the migratory arc. Dorsal POM requires high levels of TH and RA.

caudal CNC, additional signals influence PA formation (Betancur et al., 2010). Using both pharmacologic and genetic approaches, our work reveals that TH is required for anterior PA development and subsequent formation of Meckels and ceratohyal cartilage. In contrast, increased TH signaling disrupted posterior PA development, revealing the need for spatially balanced TH signaling. The rostral CNC is also patterned by homeodomain transcription factors. However, additional factors that further regulate end migration are not well characterized (Betancur et al., 2010; Minoux and Rijli, 2010). We found that TH signaling was required for ventral wave initiation, but persistently high levels of TH altered migratory paths. This finding would be consistent with the possibility that relatively high TH signaling is required for initiating ventral migration, while active inhibition of TH signaling is required for completion of migration (i.e. "TH spike"). Alternatively, steady and actively-maintained low levels of TH signaling may be necessary for proper ventral migration and subsequent craniofacial development.

In our studies, TH functioned together with RA, revealing a complex interplay between these two regulatory signaling cascades that differentially regulate caudal and rostral CNC development (Fig. 7). In caudal CNC, TH and RA had opposite effects on PA development, in part mediated by RXR signaling. TH and RA have been shown to co-regulate genes and repress activation of each other's targets (Lee et al., 1994). The sharing of response elements by TR and RAR within regulatory domains of genes may account for some overlap in function (Williams et al., 1992). Furthermore, Thraa can transcriptionally repress RAR during early zebrafish development (Essner et al., 1997). The common heterodimer partner, RXR, may also mediate this effect since inhibiting RXR prevented RA-mediated rescue of 1st and 2nd PA phenotypes of TH deficiency. Thus, differential effects of TH and RA on anterior and posterior PAs may be in part due to stoichiometric limitations in RXR available for heterodimerization.

In rostral CNC, RA appears to be a downstream target of TH, as exogenous RA restored ventral wave migration due to decreased TH signaling. However, elevated levels of TH or RA disrupted ventral wave migration, suggesting that tight spatiotemporal regulation of TH and RA levels is critical to proper development. The developing eye may be a local source for both TH and RA since *dio2*, *raldh2,* and *raldh3* are expressed in the retina in well-defined spatiotemporal patterns (Bohnsack et al., 2012; Thisse et al., 2001). Of note, RARs in the POM regulate *pitx2* expression, which is required for ocular anterior segment, optic nerve and EOM development (Bohnsack et al., 2012; Evans and Gage, 2005; Kitamura et al., 1999; Kumar and Duester, 2010; Matt et al., 2008). Interfering with TH signaling (either increased or decreased) changed the pattern of *pitx2* expression which is possibly mediated by altered RA levels. We know from our previous work that *pitx2* expression responds in spatially distinct ways to changes in RA levels (Bohnsack et al., 2012). Thus, while the total amount of *pitx2* levels may remain the same, the regional levels, which are important in the local regulation of the neural crest, can be altered by RA.

The RA and TH relationship in CNC development may have important implications on human disease. Thyroid eye disease (TED) is caused by hypertrophy, hyperplasia, and fibrosis of orbital connective tissue, fat, and EOM, all of which are derived from or organized by CNC (Bohnsack et al., 2011). Despite extensive research, the etiology of TED is poorly understood. Fibroblast proliferation, transdifferentiation, and glycosaminoglycan deposition may reflect a switch to a developmentally regressed state. The targeting of the orbit (ophthalmopathy) and skin (dermopathy) has been poorly understood, although our findings suggest a possible explanation. RA is important during embryogenesis, but adults are mostly devoid of retinoid signaling except for specific organs and anatomic locales, such as the orbit and skin. We hypothesize that high retinoid concentration, coupled with rapid and transient local alterations in TH levels that are characteristic of unstable Graves' disease, may cause CNC-derived orbital fibroblasts to reactivate a dormant embryologic program. This hypothesis is supported by the finding that radioactive iodine ablation of overactive thyroid glands can worsen the orbitopathy, possibly by causing local fluctuations in TH (Bartalena et al., 1998), although steady state levels of serum TH may remain unchanged because of the long half-life of T4. This hypothesis suggests that altering orbital retinoid biology may affect the course and severity of TO. Further studies are required to investigate the connection between RA and TH during craniofacial development and in acquired human disorders.

In summary, we report that in zebrafish, TH is required for CNC development and subsequent craniofacial and ocular morphogenesis. TH signaling functions alongside and in coordination with RA signaling in regulating PA formation and rostral neural crest migration, proliferation, and survival. These findings provide important insights into normal development, the genetics of congenital craniofacial anomalies, and disease pathogenesis.

Funding

This study was supported by T32 EY013934 from NEI of the NIH (BLB), Knights Templar Eye Foundation (BLB), Fight for Sight (BLB), Research to Prevent Blindness (AK), and K08 EY018689 from the NEI of the NIH. This research utilized Vision Research Core (P30 EY007003), and Michigan Diabetes Research and Training Center (P30 DK020572). AK is supported by Helmut F. Stern Career Development Endowed Professorship in Ophthalmology and Visual Sciences. AK acknowledges support from The Alliance for Vision Research. The Zebrafish International Resource Center is supported by Grant P40 RR012546 from the NIH NCRR. Funders had no role in study design, data collection and analysis, decision to publish, or manuscript preparation.

Acknowledgments

The authors acknowledge Mitchell Gillett for tissue processing, sectioning, and staining of methylacrylate sections and Steve Grzegorski for expert technical assistance. We thank Ronald Koenig, Peter Arvan, Peter Hitchcock, Phil Kish, and Terry Smith for helpful discussions, David Turner for pCS2-EGFP plasmid, and Tom Schilling, Mary Halloran, Simon Hughes, and Rachel Wong for zebrafish strains.

Appendix A. Supporting information

Supplementary data associated with this article can be found in the online version at http://dx.doi.org/10.1016/j.ydbio.2012.11.005.

References

Barembaum, M., Bronner-Fraser, M., 2005. Early steps in neural crest specification. Semin. Cell Dev. Biol. 16, 642–646.

Bartalena, L., Marcocci, C., Pinchera, A., 1998. On the effects of radioiodine therapy on Graves' ophthalmopathy. Thyroid 8, 533–534.

Barthel, L.K., Raymond, P.A., 2000. *In situ* hybridization studies of retinal neurons. Methods Enzymol. 316, 579–590.

Betancur, P., Bronner-Fraser, M., Sauka-Spengler, T., 2010. Assembling neural crest regulatory circuis into a gene regulatory network. Annu. Rev. Cell Dev. Biol. 26, 581–603.

Bohnsack, B.L., Gallina, D., Thompson, H., Kasprick, D., Lucarelli, M.J., Dootz, G., Nelson, C., McGonnell, I.M., Kahana, A., 2011. Development of extraocular muscles require early signals from periocular neural crest and the developing eye. Arch. Ophthalmol. 129, 1030–1041.

Bohnsack, B.L., Kasprick, D., Kish, P.E., Goldman, D., Kahana, A., 2012. A zebrafish model of Axenfeld–Rieger Syndrome reveals that *pitx2* regulation by retinoic

acid is essential for ocular and craniofacial development. Invest. Ophthalmol. Vis. Sci. 53, 7–22.
Bolande, R.P., 1974. The neurocristopathies: a unifying concept of disease arising in neural crest maldevelopment. Hum. Pathol. 5, 409–429.
Couly, G.F., Coltey, P.M., Le Douarin, N.M., 1993. The triple origin of skull in higher vertebrates: a study in quail-chick chimeras. Development 177, 409–429.
Curran, K., Raible, D.W., Lister, J.A., 2009. Foxd3 controls melanophore specification in the zebrafish neual crest by regulation of Mitf. Dev. Biol. 332, 408–417.
Deltour, L., Ang, H.L., Duester, G., 1996. Ethanol inhibition of retinoic acid synthesis as a potential mechanism for fetal alcohol syndrome. FASEB J. 10, 1050–1057.
Depew, M.J., Lufkin, T., Rubenstein, J.L., 2002. Specification of jaw subdivisions by Dlx genes. Science 298, 381–385.
Depew, M.J., Simpson, C.A., Morasson, M., Rubenstein, J.L., 2005. Reassessing the Dlx code: the genetic regulation of branchial arch skeletal pattern and development. J. Anat. 207, 501–561.
Dong, F., Sun, X., Liu, W., Ai, D., Klysik, E., Lu, M.-F., Hadley, J., Antoni, L., Chen, L., Baldini, A., Francis-West, P., Martin, J.F., 2006. Pitx2 promotes development of splanchnic mesoderm-derived branchiomeric muscle. Development 133, 4891–4899.
Dutton, K., Dutton, J.R., Pauliny, A., Kelsh, R.N., 2001. A morpholino phenocopy of the colourless mutant. Genesis 30, 188–189.
el Ghouzzi, V., Le Merrer, M., Perrin-Schmitt, F., Lajeunie, E., Benit, P., Renier, D., Bourgeois, P., Bolcato-Bellemin, A.L., Munnich, A., Bonaventure, J., 1997. Mutations of the TWIST gene in the Saethre–Chotzen syndrome. Nat. Genet. 15, 42–46.
Essner, J.J., Breuer, J.J., Essner, R.D., Fahrenkrug, S.C., Hackett, P.B., 1997. The zebrafish thyroid hormpone receptor α1 is expressed during early embryogenesis and can function in transcriptional repression. Differentiation 62, 107–117.
Evans, A.L., Gage, P.J., 2005. Expression of the homeobox gene Pitx2 in neural crest is required for optic stalk and ocular anterior segment development. Hum. Mol. Genet. 14, 3347–3359.
Gage, P.J., Suh, H., Camper, S.A., 1999. Dosage requirement of Pitx2 for development of multiple organs. Development 126, 4643–4651.
Gamborino, M.J., Sevilla-Romero, E., Munoz, A., Hernandez-Yago, J., Renau-Piqueras, J., Pinazo-Duran, M.D., 2001. Role of thyroid hormone in craniofacial and eye development using a rat model. Ophthalmic Res. 33, 283–291.
Germanguz, I., Lev, D., Waisman, T., Kim, C.H., Gitelman, I., 2007. Four twist genes in zebrafish, fish expression patterns. Dev. Dyn. 236, 2615–2626.
Gitton, Y., Heude, E., Vieux-Rochas, M., Benouaiche, L., Fontaine, A., Sato, T., Kurihara, Y., Kurihara, H., Couly, G., Levi, G., 2010. Evolving maps in craniofacial development. Semin. Cell Dev. Biol. 21, 301–308.
Golding, J.P., Dixon, M., Gassmann, M., 2002. Cues from neuroepithelium and surface ectoderm maintain neural crest-free regions within cranial mesenchyme of the developing chick. Development 129, 1095–1105.
Golding, J.P., Sobieszczuk, D., Dixon, M., Coles, E., Christiansen, J., Wilkinson, D., Gassmann, M., 2004. Roles of erbB4, rhombomere-specific and rhombomere-independent cues in maintaining neural crest-free zones in the embryonic head. Dev. Biol. 266, 361–372.
Gothe, S., Wang, Z., Ng, L., Kindblom, J.M., Barros, A.C., Ohlsson, C., Vennstrom, B., Forrest, D., 1999. Mice devoid of all known thyroid hormone receptors are viable but exhibit disorders of the pituitary-thyroid axis, growth, and bone maturation. Genes Dev. 13, 1329–1341.
Graham, A., Heyman, I., Lumsden, A., 1993. Even-numbered rhombomeres control the apoptotic elimination of neural crest cells from odd-numbered rhombomeres in the chick hindbrain. Development 119, 233–245.
Gruber, H.E., 1992. Adaptations of Goldner's Masson trichrome stain for the study of undecalcified plastic embedded bone. Biotechnic Histochem. 67, 30–34.
Higashijima, S., Okamoto, H., Ueno, N., Hotta, Y., Eguchi, G., 1997. High-frequency generation of transgenic zebrafish which reliably express GFP in whole muscles or the whole body by using promoters of zebrafish origin. Dev. Biol. 192, 289–299.
Hirano, A., Akita, S., Fujii, T., 1995. Craniofacial deformities associated with juvenile hyperthyroidism. Cleft Palate Craniofac. J. 32, 328–333.
Hong, C.-S., Saint-Jeannet, J.-P., 2005. Sox proteins and neural crest development. Semin. Cell Dev. Biol. 16, 694–703.
Howard, T.D., Paznekas, W.A., Green, E.D., Chiang, L.C., Ortiz de Luna, R.I., Garcia Delgado, C., Gonzalez-Ramos, M., Kline, A.D., Jabs, E.W., 1997. Mutations in TWIST, a basic helix–loop–helix transcription factor, in Saethre–Chotzen syndrome. Nat. Genet. 15, 36–41.
Hunt, P., Gulisano, M., Cook, M., Sham, M.H., Faiella, A., Wilkinson, D., Boncinelli, E., Krumlauf, R., 1991a. A distinct Hox code for the branchial region of the vertebrate head. Nature 353, 861–864.
Hunt, P., Whiting, J., Nonchev, S., Sham, M.H., Marshall, H., Graham, A., Cook, M., Allemann, R., Rigby, P.W., Gulisano, M., Faiella, A., Boncinelli, E., Krumlauf, R., 1991b. The branchial Hox code and its implications for gene regulation, patterning of the nervous system and head evolution. Development (Suppl. 2), 63–77.
Israel, H., Johnson, G.F., Fierro-Benitez, R., 1983. Craniofacial malformation among endemic cretins in Ecuador. J. Craniofac. Genet. Dev. Biol. 3, 3–10.
Johnston, M.C., 1966. A radioautographic study of the migration and fat of cranial neural crest cells in the chick embryo. Anat. Rec. 156, 143–155.
Karlsson, J., von Hofsten, J., Olsson, P.-E., 2001. Generating transparent zebrafish: a refined method to improve detection of gene expression during embryonic development. Mar. Biotechnol. 3, 522–527.
Kimura, C., Takeda, N., Suzuki, M., Oshimura, M., Aizawa, S., Matsuo, I., 1997. Cis-acting elements conserved between mouse and pufferfish Otx2 genes govern the expression in mesencephalic neural crest cells. Development 124 3929–3242.
Kitamura, K., Miura, H., Miyagawa-Tomita, S., Yanazawa, M., Katoh-Fukui, Y., Suzuki, R., Ohuchi, H., Suehiro, A., Motegi, Y., Nakahara, Y., Kondo, S., Yokoyama, M., 1999. Mouse Pitx2 deficiency leads to anomalies of the ventral body wall, heart, extra- and periocular mesoderm and right pulmonary isomerism. Development 126, 5749–5758.
Kohrle, J., 1999. Local activation and inactivation of thyroid hormones: the deiodinase family. Mol. Cell. Endocrinol. 151, 103–119.
Kontges, G., Lumsden, A., 1996. Rhombencephalic neural crest segmentation is preserved throughout craniofacial ontogeny. Development 122, 3229–3242.
Kumar, S., Duester, G., 2010. Retinoic acid signaling in perioptic mesenchyme represses Wnt signaling via induction of Pitx2 and Dkk2. Dev. Biol. 340, 67–74.
Kuratani, S., Matsuo, I., Aizawa, S., 1997. Developmental patterning and evolution of the mammalian viscerocranium: genetic insights into comparative morphology. Dev. Dyn. 341, 315–323.
Lampert, J.M., Holzschuh, J., Hessel, S., Driever, W., Vogt, K., von Lintig, J., 2003. Provitain A conversion to retinal via the beta,beta-carotene-15,15′-oxygenase (bcox) is essential for pattern formation and differentiation during zebrafish embryogenesis. Development 130, 2173–2186.
Lee, L.-R., Mortensen, R.M., Larson, C.A., Brent, G.A., 1994. Thyroid hormone receptor-α inhibits retinoic acid-responsive gene expression and modulates retinoic acid-stimulated neural differentiation in mouse embryonic stem cells. Mol. Endocrinol. 8, 746–756.
Lumsden, A., Sprawson, N., Graham, A., 1991. Segmental origin and migration of neural crest cells in the hindbrain region of the chick embryo. Development 113, 1281–1291.
Matsuo, I., Kuratani, S., Kimura, C., Takeda, N., Aizawa, S., 1995. Mouse Otx2 functions in the formation and patterning of rostral head. Genes Dev. 9, 2646–2658.
Matt, N., Ghyselinck, N.B., Pellerin, I., Dupe, V., 2008. Impairing retinoic acid signalling in the neural crest cells is sufficient to alter entire eye morphogenesis. Dev. Biol. 320, 140–148.
Minoux, M., Rijli, F.M., 2010. Molecular mechanisms of cranial neural crest cell migration and patterning in craniofacial development. Development 137, 2605–2621.
Noden, D.M., 1983. The role of the neural crest in patterning of avian cranial skeletal, connective, and muscle tissues. Dev. Biol. 96, 144–165.
Osumi-Yamashita, N., Ninomiya, Y., Doi, H., Eto, K., 1994. The contribution of both forebrain and midbrain crest cells to the mesenchyme in the frontomass of mouse embryos. Dev. Biol. 164, 409–419.
Prophet, E.B., Mills, B., Arrington, J.B., Sobin, L.H. (Eds.), 1992. American Registry of Pathology, Washington, D.C..
Rosa, F.W., Wilk, A.L., Felsey, F.O., 1986. Teratogen update: vitamin A congeners. Teratology 33, 355–364.
Sandell, L.L., Sanderson, B.W., Moiseyev, G., Johnson, T., Mushegian, A., Young, K., Rey, J.P., Ma, J.X., Staehling-Hampton, K., Trainor, P.A., 2007. RDH10 is essential for synthesis of embryonic retinoic acid and is required for limb, craniofacial, and organ development. Genes Dev. 21, 1113–1124.
Soo, K., O'Rourke, M.P., Khoo, P.L., Steiner, K.A., Wong, N., Behringer, R.R., Tam, P.P.L., 2002. Twist function is required for the morphogenesis of the cephalic neural tube and the differentiation of the cranial neural crest cells in the mouse embryo. Dev. Biol. 247, 251–270.
Sperber, G.H., Sperber, S.M., Guttmann, G.D., 2010. Craniofacial Embryogenetics and Development. People's Medical Publishing House, Shelton, Connecticut.
Steventon, B., Carona-Fontaine, C., Mayor, R., 2005. Genetic network during neural crest induction: from cell specification to cell survival. Semin. Cell Dev. Biol. 16, 647–654.
Stock, D.W., Ellies, D.L., Zhao, Z., Ekker, M., Ruddle, R.H., Weiss, K.M., 1996. The evolution of the vertebrate Dlx gene family. Proc. Natl. Acad. Sci. 93, 10858–10863.
Takayama, S., Hostick, U., Haendel, M., Eisen, J., Darimont, B., 2008. An F-domain introduced by alternative splicing regulates activity of the zebrafish thyroid hormone receptor α. Gen. Comp. Endocrinol. 155, 176–189.
Thisse, B., Pflumio, S., Furthauer, M., Loppin, B., Heyer, V., Degrave, A., Woehl, R., Lux, A., Steffan, T., Charbonnier, X.Q., Thisse, C., 2001. Expression of the zebrafish genome during embryogenesis. ZFIN Direct Data Submission.
Trainor, P.A., 2005. Specification of neural crest cell formation and migration in mouse embryos. Semin. Cell Dev. Biol. 16, 683–693.
Walpita, C.N., Crawford, A.D., Darras, V.M., 2010. Combined antisense knockdown of type 1 and type 2 iodothyronine deiodinases disrupts embryonic development in zebrafish (*Danio rerio*). Gen. Comp. Endocrinol. 166, 134–141.
Walpita, C.N., Crawford, A.D., Janssens, E.D.R., Van der Geyten, S., Darras, V.M., 2009. Type 2 iodothyronine deiodinase is essential for thyroid hormone-dependent embryonic development and pigmentation in zebrafish. Endocrinology 150, 530–539.
White, R.M., Sessa, A., Burke, C., Bowman, T., LeBlanc, J., Ceol, C., Bourque, C., Dovey, M., Goessling, W., Burns, C.E., Zon, L.I., 2008. Transparent adult zebrafish as a tool for *in vivo* transplantation analysis. Cell Stem Cell 2, 183–189.
Williams, G.R., Harney, J.W., Moore, D.D., Larsen, P.R., Brent, G.A., 1992. Differential capacity of wild type promoter elements for binding and trans-activation by retinoic acid and tyroid hormone receptors. Mol. Endocrinol. 6, 1527–1537.
Yeo, G.H., Cheah, F.S., Jabs, E.W., Chong, S.S., 2007. Zebrafish twist1 is expressed in craniofacial, vertebral, and renal precursors. Dev. Genes Evol. 217, 783–789.
Yonkers, M.A., Ribera, A.B., 2009. Molecular components underlying nongenomic thyroid hormone signaling in embryonic zebrafish neurons. Neural Dev. 4.
Zhang, j., Lazar, M.A., 2000. The mechanism of action of thyroid hormones. Annu. Rev. Physiol. 62, 439–466.